PHYSICAL REVIEW B VOLUME 25, NUMBER 2 15 FEBRUARY 1982

Inelastic neutron measurement of phonons in graphite-alkali intercalation compounds

H. Zabel
Department of Physics and Materials Research Laboratory, University of Illinois at Urbana-Champaign, Urbana, Illinois 61801

A. Magerl
National Measurement Laboratory, National Bureau of Standards, Washington, D. C. 20234 and Institut Laue-Langevin, 156X F-38042 Grenoble-Cedex, France
(Received 22 September 1981)

Neutron spectroscopic studies of the [001] L-phonon branches in graphite-alkali intercalation compounds C_xM ($x=8$, 24, 36; M denotes K, Rb, Cs) have been undertaken. In all cases zone-folding effects as well as frequency gaps at the center and boundary of the Brillouin zone have been observed. The phonon branches of all stages and compounds measured are well described by one-dimensional lattice-dynamical models: The alkali-graphite interplanar interaction is mediated by an electronic shell, while the interior graphite-graphite interaction is represented by Born—von Kármán force constants. Sound velocities and elastic constants of the intercalation compounds are derived from the acoustical-phonon branches.

I. INTRODUCTION

In the present paper we report on a systematic neutron spectroscopic study of [001] L-phonon dispersions in alkali-graphite intercalation compounds C_xM ($x=8$, 24, 36; M denotes K, Rb, Cs). In pristine graphite the [001] L-phonon dispersion can be described—to a good approximation—by only nearest-neighbor harmonic force constants between the basal planes.[1,2] Upon intercalation with alkali layers the symmetry, mass, and interplanar interactions change. The aim of this paper is to describe the effect of these changes on the [001] L-phonon branches.

For the study of phonons, graphite intercalation compounds (GIC's) are unique among other layered materials because of the following reasons:

(i) The structure of the basal planes is relatively simple, containing only C atoms [Fig. 1(a)].

(ii) A large variety of atoms or molecules can readily be intercalated.

(iii) High-stage n GIC's can be prepared, with a high degree of sequential order of graphite and intercalated planes, where n describes the number of graphite planes between two intercalated planes [Fig. 1(b)].

(iv) The physical properties of the parent lattice have been extensively studied and are very well known.[3]

A disadvantage of GIC's is the limited size of single crystals. So far they had been used only for diffraction studies[4] and phase transitions[5] but they are too small for inelastic neutron scattering experiments.

In the following we will confine our discussion to the donor compounds of alkali metals in graphite. With respect to the c axis, which is our concern here, the dissolved alkali atoms cause three main structural changes of the graphite host lattice:

(1) The alkali atoms intercalate in a regular fashion so that an intercalated layer is followed by a constant number of graphite planes.

(2) Alkali layers are always flanked by equivalent carbon planes, thereby causing a rearrangement of the sequential order of the graphite planes.

(3) The distance between adjacent graphite planes increases considerably (from 3.35 in pure graphite to 5.34 for K and 5.93 for Cs) upon intercalation, while the distance between interior graphite layers stays almost the same as in pure graphite.

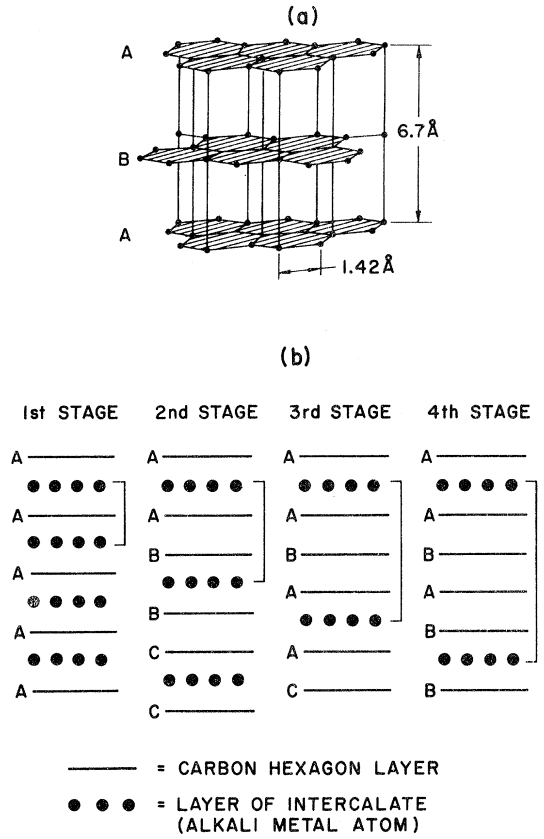

FIG. 1. (a) Structure of pristine graphite. (b) Stacking sequence of carbon and alkali layers in stage-1 to stage-4 compounds.

Thus, along the c axis the structure of alkali GIC's (AGIC's) can be considered as being mass and spacing modulated, causing c-axis lattice parameters as long as 52 Å. This in turn results in a reduction of the Brillouin zone (BZ) in the c direction. However, since the [001] L phonons are not sensitive to the stacking sequence of graphite and alkali planes along the [001] direction, the actual repeat distance I_c is determined only by the nearest distance between two alkali planes. The mass modulation causes energy gaps to open up between all phonon branches both at the BZ center and boundary, while the spacing modulation causes a rapidly changing neutron inelastic structure factor from one BZ to the next.

The phonon dispersion is also affected by the changed interplanar coupling constants. Intercalation takes place in between the van der Waals gaps of graphite planes, thereby changing the nature of the bonding between the planes. For instance, the graphite-alkali interplanar coupling may be described by a screened Coulomb interaction via electron transfer from the alkali layer to the adjacent graphite planes.[6]

In the past lattice dynamical properties of GIC's have been studied extensively by Raman scattering[7,8] and infrared reflectance.[9] Those studies are focused on the high-frequency intralayer graphite modes E_{2g} and E_{1u} at the BZ center and show directly the influence of the charge transfer on the mode frequency. Within the past year the interest in lower-energy modes in GIC's increased considerably. Besides an earlier neutron scattering study of the [001] L modes in C_8 Rb,[10] there have been recently reports on Raman scattering studies of rigid-layer shearing modes in graphite-potassium[11] and graphite-rubidium[12] compounds, neutron scattering studies of collective alkali in-plane modes,[13] and [001] L modes of the acceptor compound graphite-$FeCl_3$.[14] The authors recently reported on a first inelastic neutron study to show zone-folding effects along with opening of frequency gaps between acoustic and optic [001] L modes in $C_{36}K$.[15] We have extended this study to different stages and alkali intercalants in order to get a systematic overview of the dependence of the [001] L-phonon dispersion on structure, mass, and interplanar coupling constants. AGIC's are particularly suitable for this type of study since the intercalates behave as rigid monolayers and the results are not obscured by internal modes as might be the case for molecular intercalants in acceptor compounds. With respect to [001] L phonons, the AGIC's can be considered as a linear array of graphite and alkali planes that vibrate along the c direction. Since this vibration of planes as an entirety is independent of the in-plane orientation, the use of pyrolytic graphite with random a and b axes, instead of single crystals, is not disadvantageous. A first report of some of the results on the [001] L-phonon dispersions in AGIC's has been given elsewhere.[16]

II. EXPERIMENTAL

We used pyrolytic graphite (PG) as well as highly oriented pyrolytic graphite (HOPG) with different dimensions and mosaic spreads. The samples were intercalated with alkali atoms in a two-stage furnace in the usual manner. The alkali metals used were purchased from Alpha Division and A. D. Mackay with a stated purity of 99.9%.

TABLE I. Sample Properties. PG denotes pyrolytic graphite and HOPG denotes highly oriented pyrolytic graphite.

Compound	Pristine graphite material	Mosaic spread before intercalation	Mosaic spread after intercalation	Sample housing	Sample volume (cm^3)	Coherent scattering length density of alkali layers ($\times 10^{12}$ cm)[a]
$C_{36}K$	PG	6°	8°	Aluminum	50	0.031
$C_{24}K$	PG	6°	11°	Quartz	7	0.031
$C_{24}Rb$	PG	6°	11°	Quartz	6	0.059
$C_{24}CS$	PG	6°	11°	Quartz	7	0.046
C_8K	PG	6°	12°	Quartz	8	0.046
C_8Cs	HOPG	0.8°	2.1°	Quartz	1.2	0.068
	HOPG	0.8°				0.665

[a]Coherent scattering of alkali atoms multiplied by in-plane concentration (data taken from Ref. 26).

Stage and homogeneity of each compound were determined by x-ray and neutron elastic (00l) scans. Relevant parameters of the samples before and after intercalation are summarized in Table I.

Constant-Q scans were performed using triple-axis spectrometers at the National Bureau of Standards research reactor. HOPG was used as monochromator and analyzer. Spectra were taken with fixed incident energy, set between 13.7 and 35 meV, depending on the phonon modes. The majority of the measurements reported here were carried out at room temperature. However, the [001] L-phonon dispersion of $C_{36}K$ has been studied between 80 and 300 K as well.

III. RESULTS

The [001] L-phonon energies obtained at C_8K, $C_{24}K$, $C_{36}K$, $C_{24}Rb$, C_8Cs, and $C_{24}Cs$ are plotted in Fig. 2 and listed in Table II. For completeness we have included in Fig. 2 the [001] L-phonon energies of C_8Rb, as determined by Ellenson *et al.*[10] The phonon wave vectors are given in units of the identity period I_c, neglecting the stacking sequence of the graphite and/or alkali planes.

We were able to measure all $n+1$ longitudinal branches in each stage-n compound: one acoustical branch and n optical branches. Note that in spite of the small structure factor we succeeded in measuring the uppermost optical branch in $C_{36}K$, which was missing in Ref. 15. Mode splittings could be clearly resolved for the compounds C_8K, $C_{24}K$, $C_{36}K$, $C_{24}Rb$, and C_8Cs, whereas no splitting was observable in $C_{24}Cs$.

The splittings at the BZ center and boundary in stages $n \geq 2$ are caused by different area-mass densities of graphite and alkali layers, as well as by different interlayer coupling constants between graphite-alkali and graphite-graphite planes. However, in stage-1 compounds by symmetry considerations only differences in the area-mass densities are responsible for the observed frequency gaps. The mass dependence of the phonon dispersions can be best seen in the sequence of stage-1 compounds: Stage-1 K with the lightest area-mass density exhibits the highest optical branch, followed by Rb and Cs. Note, however, that for stage-1 Cs the carbon planes have a smaller area-mass density than the Cs planes. Remarkable also is that the optical branch of stage-1 K has less dispersion than those of Rb and Cs. In addition, it flattens with increasing stage number, which is indicative for a localized mode behavior of the light potassium planes in high-stage compounds.

In general, the highest optical branch is characterized by a large and predominant amplitude of the planes with the smaller area-mass density. These are usually the alkali planes. In spite of their large amplitude, the inelastic structure factor is small, mainly because of the small coherent scattering length of the alkali planes and the high energy of the optical branch, and therefore are normally hard to observe. However, in stage-1 C_8Cs the situation is reversed, as already mentioned. Thus, in C_8Cs the structure factor of the optical branch is determined by the larger coherent scattering length of the carbon atoms and their higher in-plane density, and its measurement is therefore much facilitated. In Table I we have list-

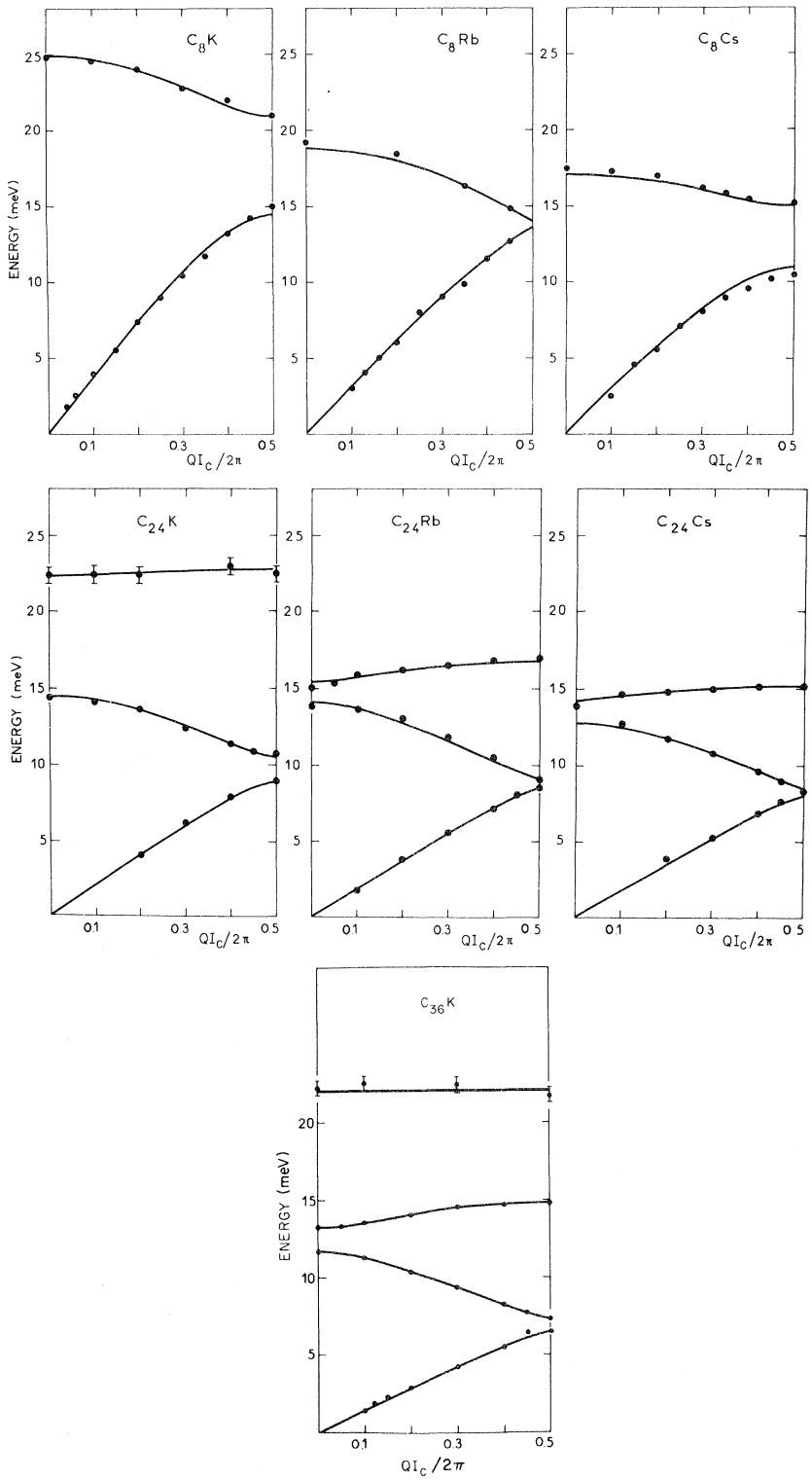

FIG. 2. Measured phonon energies for [001] L modes in alkali-graphite intercalation compounds at 296 K. The phonon energies of C_8Rb (Ref. 10) have been included here for completeness. Full lines are best fits with one-dimensional ion-shell models. For details, see text.

TABLE II. Energies (meV) of normal modes in alkali-graphite intercalation compounds (a) C_8K, (b) $C_{24}K$, (c) $C_{36}K$, (d) $C_{24}Rb$, (e) C_8Cs, and (f) $C_{24}Cs$ at 296 K, propagating in the [001] direction.

(a) C_8K

$\frac{qI_c}{2\pi}$	LA	LO
0.0		24.75±0.25
0.04	1.75±0.2	
0.06	2.50±0.15	
0.1	3.90±0.15	24.50±0.25
0.15	5.50±0.15	
0.2	7.40±0.15	24.00±0.5
0.25	9.00±0.15	
0.3	10.5 ±0.15	22.75±0.5
0.35	11.75±0.1	
0.40	13.25±0.1	22.00±0.5
0.45	14.25±0.1	
0.5	15.00±0.1	21.00±0.5

(b) $C_{24}K$

$\frac{qI_c}{2\pi}$	LA	1. LO	2. LO
0.0		14.4 ±0.1	22.4±0.5
0.1		14.1 ±0.1	22.5±0.7
0.2	4.10±0.15	13.65±0.1	22.4±0.4
0.3	6.2 ±0.15	12.35±0.1	
0.4	7.9 ±0.1	11.4 ±0.1	23.0±0.7
0.45		10.87±0.1	
0.5	8.96±0.1	10.76±0.1	22.5±0.5

(c) $C_{36}K$

$\frac{qI_C}{2\pi}$	LA	1. LO	2. LO	3. LO
0		11.68±0.3	13.21±0.2	22.2±0.5
0.05			13.33±0.3	
0.10	1.40±0.1	11.30±0.2	13.54±0.2	22.5±0.7
0.12	1.9 ±0.1			
0.15	2.31±0.1			
0.20	2.91±0.1	10.41±0.15	14.06±0.15	
0.30	4.23±0.1	9.41±0.1	14.55±0.15	22.4±0.5
0.40	5.46±0.1	8.36±0.1	14.70±0.1	
0.45	6.44±0.1	7.78±0.1		
0.50	6.53±0.15	7.36±0.15	14.79±0.1	21.7±0.7

ed the coherent scattering length densitites of the alkali planes.

In anticipation of a coupling of the alkali order-disorder phase transition to the phonon dispersion, we have measured the [001] L-phonon branches of $C_{36}K$ between 80 K and room temperature. The alkali order-disorder transition in $C_{36}K$ is reported to appear at around 130 K.[17] Measurements have been taken in steps of 20 K and the BZ extension was corrected each time for thermal expansion. We have not observed any change across the phase transition, neither in the phonon energies nor in

TABLE II. (continued.)

(d) $C_{24}Rb$

$\frac{qI_c}{2\pi}$	LA	1. LO	2. LO
0.0	0	13.8 ±0.3	15.0 ±0.1
0.05			15.35±0.25
0.10	1.75±0.1	13.6 ±0.2	15.85±0.25
0.20	3.8 ±0.1	13.0 ±0.2	16.1 ±0.25
0.30	5.5 ±0.1	11.75±0.25	16.5 ±0.5
0.40	7.1 ±0.1	10.5 ±0.1	16.8 ±0.3
0.45	8.0 ±0.1		
0.50	8.5 ±0.15	9.0 ±0.3	17.0 ±0.1

(e) C_8Cs

$\frac{qI_c}{2\pi}$	LA	LO
0.0		17.5 ±0.1
0.1	2.5 ±0.2	17.3 ±0.1
0.15	4.61±0.2	
0.20	5.6 ±0.15	17.0 ±0.12
0.25	7.12±0.1	
0.3	8.12±0.1	16.25±0.12
0.35	9.0 ±0.1	15.87±0.12
0.4	9.6 ±0.1	15.5 ±0.12
0.45	10.25±0.1	
0.5	10.5 ±0.1	15.25±0.12

(f) $C_{24}Cs$

$\frac{qI_c}{2\pi}$	LA	1. LO	2. LO
0.0		13.90±0.1	13.90±0.1
0.1		12.70±0.15	14.64±0.1
0.2	3.87±0.1	11.65±0.1	14.76±0.1
0.3	5.32±0.1	10.70±0.12	14.95±0.1
0.4	6.87±0.1	9.5 ±0.12	15.12±0.1
0.45	7.63±0.1	8.92±0.1	
0.5	8.3 ±0.2	8.3 ±0.2	15.15±0.1

the inelastic structure factors.

IV. DISCUSSION

A. Phonon dispersion and phonon models

None of the measured phonon dispersions can consistently be interpreted by a simple one-dimensional Born–von Kármán model, as proposed earlier.[15] The discrepancy becomes obvious in $C_{36}K$: A fit of the lower three branches predicts an uppermost flat branch at 25 meV. The experiments indeed reveal a dispersionless branch, however, at the considerably lower energy of 22.5±0.5 meV. The addition of longer-range force constants between alkali and alkali planes, alkali and second-nearest-neighbor graphite planes, or graphite and graphite planes adjacent to an alkali plane is likewise not successful. This is discussed in more detail in Ref. 16. Clearly, with a larger number of force constants of increasing range the measured phonon branches could finally be reproduced. However, the physical interpretation of such a model would be unsatisfactory. A simpler and clearer description of the phonon dispersions can be derived from a mixed nearest-neighbor Born–von Kármán and shell model,[18] as shown in

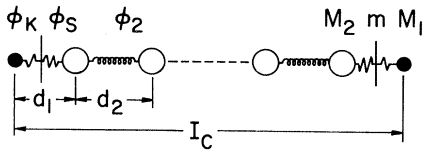

FIG. 3. Schematic representation of the one-dimensional shell model for [001] L phonons in stage-n compound. d_1 and d_2 are the distances between alkali-graphite and graphite-graphite planes, respectively. Ic is the repeat distance in c direction, disregarding any stacking. M_1 and M_2 are the alkali and graphite area-mass respectively, densities, and m is the electron mass density, which is extrapolated to zero. ϕ_K is the core shell, ϕ_S is the shell-graphite, and ϕ_2 the interior graphite-graphite force constant.

Fig. 3. In this model, each alkali mass point is replaced by a heavy core and a shell with zero mass (adiabatic approximation). ϕ_K is the force constant between alkali core and shell, and ϕ_S is the force constant between the shell and adjacent graphite layers. The interaction between the interior graphite planes is still treated by a nearest-neighbor Born—von Kármán model, with ϕ_2 as the only force constant, as in pristine graphite. The insertion of an electronic shell between alkali and graphite planes is justified by the charge transfer from intercalant to graphite planes in donor compounds, which makes the alkali-graphite bonding ionic in character.[19]

The alkali core-shell interaction is short in range, but due to the polarization of the electrons long in behavior. As compared to the nearest-neighbor Born—von Kármán model, the mixed model therefore yields lower phonon energies for the upper branches, while leaving the lower branches almost unaffected. In particular, the initial slope of the acoustic branch remains unchanged. This feature makes a good fit to the experimental data possible, as shown by the full lines in Fig. 2. A list of the fit parameter (two for stage 1, ϕ_K and ϕ_S; three for stages $n \geq 2$, ϕ_K, ϕ_S, and ϕ_2) is given in Table III.

Here and in the following discussion we assume "classical" stoichiometric compositions, even though recent experiments have cast some doubt on this assumption.[20] However, deviations from stoichiometry normally are very small (less than $\pm 2\%$) and do not influence our principle conclusions.

From Table III it can be seen that the force constants ϕ_2 are increased by about 7% for all stage-2 compounds, as compared to pristine graphite. We take this as a clear indication for a long-range influence of the intercalation on the interplanar binding forces. Additionally, the insertion of an electronic shell causes a polarization of the one-dimensional chain equivalent to longer-range interactions between the atoms as already mentioned. It may be speculated that these effects have some implication on the highly ordered stacking sequence of GIC's. The force constants ϕ_K are roughly an order of magnitude larger than ϕ_S, while ϕ_S is about 10—20% larger than ϕ_2 for stages $n \geq 2$ compounds. Remarkable also is the tremendous

TABLE III. Best-fit force constants in dyn/cm for alkali-graphite intercalation compounds for a shell model. ϕ_K, ϕ_S and ϕ_2 represent the alkali-core—electronic-shell interaction, the bonding-graphite-layer—electronic-shell interaction, and the graphite-graphite interaction, respectively. ϕ_2 for pristine graphite is equivalent to the Born—van Kármán interplanar coupling constant. See also Fig. 3.

	ϕ_K	ϕ_S	ϕ_2
Pristine graphite			2800
$C_{36}K$	22460±2350	3510±80	2885±30
$C_{24}K$	21120± 300	3690±65	3000±50
$C_{24}Rb$	19870± 570	3350±35	2950±80
$C_{24}Cs$	15650±1320	3420±65	3065±65
C_8K[a]	37770±1150	3232±10	
C_8Rb[a]	33020±4700	3040±50	
C_8Cs[a]	20940±1700	3480±50	

[a]For an easy comparison the results for the stage-1 compounds have been multiplied by $\frac{2}{3}$. Thus the values shown represent C_{12} alkali compounds.

increase of ϕ_S from stage-2 to stage-1 compounds. This strengthening of the interplanar coupling is also expressed in larger sound velocities and elastic constants C_{33}, to be discussed below. In this context it is worthwhile to remind the reader that stage-1 compounds form a three-dimensional solid with alkali 2×2 in-plane order,[21] while in stages $n \geq 2$ the alkali atoms are disordered with a two-dimensional liquidlike structure factor at room temperature.[5,22,23]

In summary, the force constants obtained with the one-dimensional mixed Born—von Kármán and shell model indicate an overall strenghtening of the interplanar interaction. This observation is contrasted by recent neutron results, which seem to indicate a weakening of the interplanar coupling in acceptor compounds.[14]

B. Macroscopic elastic properties

The sound velocities V along the c axis and the elastic constants C_{33} via $V^2\rho = C_{33}$ have been calculated from the initial slope $\Delta w/\Delta q$ of the acoustical branches as obtained from the fits with our model. The volume-mass density ρ depends on the stage-n and area-mass density of the alkali atoms in the specific compound, and is given by

$$\rho = \frac{4p\,(nA_c + \alpha A_a)}{\sqrt{3} I_c^n a^2} ,$$

where p is the proton mass, α is the in-plane atomic alkali concentration, A_c and A_a are the atomic weights of carbon and alkali atoms, respectively, I_n^c is the identity period of stage-n compounds, and a is the graphite in-plane lattice parameter. All values obtained for V and C_{33} are tabulated in Table IV and compared with literature values where available.

A distinct increase in sound velocities and elastic constants of about 35% is noticeable in stage-1 compounds, while the higher-stage compounds have almost the same V and C_{33} as pure graphite. These results reflect the increased graphite-alkali interplanar coupling constants due to charge transfer along the c axis, which is most pronounced in stage-1 compounds but averaged out in stage $n \geq 2$ compounds, partly because of the smaller alkali concentration and partly by the contribution of the inner graphite planes.

Our values for the elastic constant C_{33}, derived from the [001] L-phonon dispersion, agree fairly well with recent x-ray c-axis compressibility measurements of stage-1 compounds. In the latter work an increase of C_{33} (decrease of the compressibility) was also observed. However, we have seen no indication for softening in $C_{24}K$ as reported by Wada *et al.*[24,25] We attribute this discrepancy to the different experimental methods. While the initial slope of the acoustic [001] L mode is a direct measure of the elastic constant C_{33}, the c axis compressibility $K_c = (1/c_0)(\partial c/\partial p)_{p0}$ may be influ-

TABLE IV. Values for sound velocities V and elastic constants C_{33} as calculated from the initial slope $\Delta w/\Delta q$ of the acoustical branches as obtained from the fits of our model.

	I_c (Å)	Area-mass density (amu)	ρ (g/cm^3)	$V\times10^5$ (cm/sec)	$C_{33}\times10^{11}$ (dyn/cm^2)	C_{33} or $K_c\times10^{11}$ (dyn/cm^2)
Pristine graphite	3.355±0.001	12.0	2.28	4.0[b]	3.71±0.05[b]	3.71±0.05[b]
$C_{36}K$	12.07 ±0.005	3.26	2.07	4.19±0.05	3.53±0.10	
$C_{24}K$	8.74 ±0.005	3.26	1.98	4.36±0.05	3.75±0.10	2.10±0.5[b]
$C_{24}Rb$	9.055±0.002	7.12	2.19	4.09±0.05	3.55±0.10	
$C_{24}Cs$	8.37 ±0.005	11.07	2.38	3.61±0.07	3.10±0.13	
C_8K	5.34 ±0.005	4.875	2.012	4.91±0.07	4.85±0.14	4.69±0.02[c]
C_8Rb	5.64[a]	10.68	2.56	4.35[a]	4.84[a]	4.13±0.02[d]
C_8Cs	5.929±0.001	16.61	3.07	4.36±0.1	5.83±0.12	6.41±0.02[d]

[a]Reference 10.
[b]Reference 2.
[c]Reference 24.
[d]Refernce 25.

enced by the creation of dislocations under high pressures, which is impossible in the case of the inelastic neutron data.

V. CONCLUSION

We have determined the [001] L-phonon branches of several alkali GIC's. The [001] L modes are polarized normal to the graphite and alkali planes and therefore can be considered as the motion of a one-dimensional chain of stacked graphite and alkali layers. To our knowledge, the [001] L modes of alkali GIC's present the only example of a linear chain, whose properties can artificially be changed on an atomic scale. Depending on the type of alkali chosen and the stage of the compound, the mass, symmetry and interplanar coupling constants can be altered. By inelastic neutron scattering we were able to determine the whole dispersion of all [001] L acoustical and optical phonon branches. We have shown that a mixed one-dimensional Born—von Kármán and shell model provides a consistent description of all [001] L modes in donor GIC's. From the model and obtained force constants we conclude that the range as well as the strength of the interplanar interaction increases considerably upon intercalation with alkali atoms. From the initial slope of the acoustical branches we have deduced macroscopic elastic properties of the AGIC's, otherwise difficult to measure.

ACKNOWLEDGMENTS

We are grateful to J. J. Rush and J. M. Rowe for valuable discussions and to A. W. Moore for providing HOPG materials used in this study. This work was supported in part by the U. S. Department of Energy under Contract No. DE-AC02-76ER1198, the Research Corporation, and the University of Illinois Research Board.

[1]G. Dolling and B. N. Brockhouse, Phys. Rev. 128, 1120 (1962).
[2]R. Nicklow, N. Wakabayashi, and H. G. Smith, Phys. Rev. B 5, 4951 (1972).
[3]A. R. Ubbelohde and T. A. Lewis, *Graphite and Its Crystal Compounds* (Clarendon, Oxford, 1960).
[4]D. Guérard and A. Hérold, Carbon 13, 337 (1975).
[5]R. Clarke, N. Caswell, S. A. Solin, and P. M. Horn, Phys. Rev. Lett. 43, 2018 (1979); M. Mori, S. C. Moss, Y. M. Jan, and H. Zabel Phys. Rev. B 25, (1982).
[6]F. Batallau, J. Bok, I. Rosenman, and J. Merlin, Phys. Rev. Lett. 41, 330 (1978); L. Pietronero, S. Strässler, H. R. Zeller, and M. J. Rice, *ibid.* 41, 763 (1978).
[7]P. C. Eklund, G. Dresselhaus, M. S. Dresselhaus, and J. E. Fischer, Phys. Rev. B 21, 4705 (1980).
[8]R. J. Nemanich, S. A. Solin, and D. Guérard, Phys. Rev. B 16, 2965 (1977).
[9]R. J. Nemanich and S. A. Solin, Solid State Commun. 23, 417 (1977).
[10]W. D. Ellenson, D. Semmingsen, D. Guérard, D. G. Onn, and J. E. Fischer, Mater. Sci. Eng. 31, 137 (1977).
[11]N. Wada, M. V. Klein, and H. Zabel, in *Proceedings of the International Conference on the Physics of Intercalation Compounds, Trieste, Italy, 1981,* Vol. 38 of *Springer Series in Solid State Sciences,* edited by L. Pietronero and E. Tosatti (Springer, Berlin, 1981).
[12]P. C. Eklund, in *Proceedings of the International Conference on the Physics of Intercalation Compounds, Trieste, Italy, 1981,* Ref. 11.
[13]W. A. Kamitakahara, N. Wada, and S. A. Solin (unpublished).
[14]J. D. Axe, C. F. Majkrzak, L. Passell, S. K. Satija, G. Dresselhaus, and H. Mazurek, in *Proceedings of the Fifteenth Biennial Conference on Carbon, Pennsylvania, 1981* (in press).
[15]A. Magerl and H. Zabel, Phys. Rev. Lett. 46, 444 (1981).
[16]A. Magerl and H. Zabel, in *Proceedings of the International Conference on the Physics of Intercalation Compounds, Trieste, Italy, 1981,* Ref. 11.
[17]Y. M. Jan, M. Mori, S. C. Moss, Bull. Amer. Phys. Soc. 26, 452 (1981) (unpublished).
[18]R. A. Cowley, W. Cochran, B. N. Brockhouse, A. D. B. Woods, Phys. Rev. 131, 1030 (1963).
[19]For a review of the electronic properties see M. S. Dresselhaus and G. Dresselhaus, Adv. Phys. 30, 139 (1981).
[20]S. Y. Leung, C. Underhill, G. Dresselhaus, T. Krapchev, R. Ogilvie, and M. S. Dresselhaus, Phys. Lett. A 76A, 89 (1980); N. Caswell, Phys. Rev. B 22, 6308 (1980).
[21]P. Lagrange, D. Guérard, A. Hérold, Ann. Chim. (Rome) 3, 143 (1978).
[22]H. Zabel, S. C. Moss, N. Caswell, and S. A. Solin, Phys. Rev. Lett. 43, 2022 (1979).
[23]J. B. Hastings, W. D. Ellenson, and J. E. Fischer, Phys. Rev. Lett. 42, 1552 (1979).
[24]N. Wada, R. Clarke, and S. A. Solin, Solid State Commun. 25, 675 (1980).
[25]N. Wada, Phys. Rev. B 24, 1065 (1981).
[26]G. E. Bacon, *Neutron Diffraction* (Clarendon, Oxford, 1975).